Nonclassical oscillations in pre- and post-selected quantum walks

Xiao-Xiao Chen,[1] Zhe Meng,[1] Jian Li,[1] Jia-Zhi Yang,[1] An-Ning Zhang,[1,*] Tomasz Kopyciuk,[2] and Paweł Kurzyński[3,†]

[1]*Center for Quantum Technology Research and Key Laboratory of Advanced Optoelectronic Quantum Architecture and Measurements (MOE), School of Physics, Beijing Institute of Technology, Haidian District, Beijing 100081, People's Republic of China*

[2]*Faculty of Physics, Adam Mickiewicz University, Uniwersytetu Poznańskiego 2, 61-614 Poznań, Poland*

[3]*Institute of Spintronics and Quantum Information, Faculty of Physics, Adam Mickiewicz University, Uniwersytetu Poznańskiego 2, 61-614 Poznań, Poland*

(Received 31 January 2021; accepted 9 July 2021; published 28 July 2021)

Quantum walks are counterparts of classical random walks. They spread faster, which can be exploited in information processing tasks, and constitute a versatile simulation platform for many quantum systems. Yet, some of their properties can be emulated with classical light. This raises a question: which aspects of the model are truly nonclassical? We address it by carrying out a photonic experiment based on a pre- and post-selection paradox. The paradox implies that if somebody could choose to ask either if the particle is at position $x = 0$ at even time steps or at position $x = d$ $(d > 1)$ at odd time steps, the answer would be positive, no matter the question asked. Therefore, the particle seems to undergo long distance oscillations despite the fact that the model allows it to jump one position at a time. We translate this paradox into a Bell-like inequality and then into a contextuality witness. Finally, we experimentally verify this witness up to eight standard deviations.

DOI: 10.1103/PhysRevA.104.012220

I. INTRODUCTION

We study the nonclassicality of a discrete-time quantum walk (DTQW) [1,2], a quantum counterpart of the quintessential random walk, in which the walker and the driving coin are quantum systems capable of becoming superposed and interfering. The interference is responsible for a behavior that strikingly differs from the classical random diffusion. DTQWs spread ballistically faster and their spatial probability distribution is far from Gaussian.

Despite the fact that DTQWs can simulate various quantum systems and their ballistic spreading properties are used in a number of information processing algorithms [3–6], it is possible to emulate their behavior with classical light [7–10]. More precisely, if instead of a particle, such as a photon, one used a classical coherent light beam in a DTQW experiment, the beam's amplitude would mimic the walker's probability amplitude. Does this mean that there is nothing nonclassical about DTQWs? The only difference between the two scenarios seems to lie in the measurement. In the case of the classical light, one performs a single experiment that yields an intensity distribution at all positions. In the quantum case, one performs many experiments, each resulting in a single click at a random position, and only later one evaluates a probability distribution that matches the classical intensity pattern. Although the two methods of obtaining the probability distribution seem equivalent, it is known that single-partite nonclassical properties resulting from clicks become classically explainable if one performs collective intensity measurements on more than one indistinguishable particle [11]. Therefore, in order to expose any nonclassicality in DTQWs, one should focus on single-particle clicks and examine if some of their properties lack a classical description.

The lack of a classical description means that measurements on a system cannot be described by a particular type of hidden variable (HV). HVs provide a classical probabilistic description of measurements [12] under some physically motivated assumptions. The most common physically motivated assumptions are locality [13] (a measurement in one location does not affect a measurement in some other, spatially separated location), noncontextuality [14] (an outcome of one measurement does not depend on which other compatible measurement is performed together with it), and so-called macrorealism [15] (a measurement at time t_0 does not influence the outcome of a measurement at some later time t_1).

In [16], it was experimentally confirmed that DTQWs do not meet the macrorealism assumption. Here, we experimentally show that DTQWs do not meet the noncontextuality assumption under an assumption that some measurement outcomes are exclusive. We do this by designing a Bell-like inequality [13] and then transforming it into a contextuality witness. Next, we verify this witness with experimentally obtained measurement data. The inequality and the witness are based on a recent logical pre- and post-selection (LPPS) paradox designed by some of the authors [17]. Notice that LPPS paradoxes were shown to be proofs of contextuality [18,19], and hence if some system admits such a paradox, it is nonclassical in the sense that it is contextual [14].

II. MODEL AND RESULTS

A. Discrete-time quantum walks model

We consider a DTQW on a one-dimensional (1D) lattice. The system's state is given by $|x\rangle \otimes |c\rangle$, where $x \in \mathbb{Z}$ is the

*anningzhang@bit.edu.cn
†pawel.kurzynski@amu.edu.pl

position of the walker and $c = \pm$ represents two states of the coin. A single step is described by an operator $U = S(\mathbb{1} \otimes C)$, where S is the conditional translation,

$$S|x\rangle \otimes |\pm\rangle = |x \pm 1\rangle \otimes |\pm\rangle, \tag{1}$$

and C is the coin-toss operation that we choose to be $C = NOT$, i.e., $C|\pm\rangle = |\mp\rangle$.

The above evolution is periodic and the period is just two steps. It can be rewritten as

$$U = S_+ + S_-, \tag{2}$$

where $S_+ = \sum_x |x+1\rangle\langle x| \otimes |+\rangle\langle -|$ and $S_- = S_+^\dagger$. A state $|x\rangle \otimes |\pm\rangle$ after the first step becomes $|x \mp 1\rangle \otimes |\mp\rangle$, but after the second step, it returns to $|x\rangle \otimes |\pm\rangle$. Due to reasons that will be explained in a moment, we are interested in an initial state that is a particular superposition of position and coin states. We are going to initialize the system (pre-select it) in the state

$$|\mathrm{pre}(0)\rangle = \frac{1}{\sqrt{5}}[|0\rangle \otimes |-\rangle + (|2\rangle + |4\rangle) \otimes (|-\rangle + |+\rangle)]. \tag{3}$$

After the first step, the system's state is

$$|\mathrm{pre}(1)\rangle = \frac{1}{\sqrt{5}}[(|1\rangle + |3\rangle) \otimes (|-\rangle + |+\rangle) + |5\rangle \otimes |+\rangle], \tag{4}$$

and after the second step, it is

$$|\mathrm{pre}(2)\rangle = |\mathrm{pre}(0)\rangle. \tag{5}$$

Once the two steps are implemented, we are going to measure if the system is in the state (post-select it),

$$|\mathrm{post}(2)\rangle = \frac{1}{\sqrt{5}}[|0\rangle \otimes |-\rangle + (|2\rangle + |4\rangle) \otimes (|-\rangle - |+\rangle)]. \tag{6}$$

The probability of post-selection is

$$|\langle \mathrm{post}(t)|\mathrm{pre}(t)\rangle|^2 = \tfrac{1}{25}. \tag{7}$$

Finally, notice that the post-selected state can, in principle, be evolved backwards in time,

$$|\mathrm{post}(1)\rangle = \frac{1}{\sqrt{5}}[(|1\rangle + |3\rangle) \otimes (|+\rangle - |-\rangle) + |5\rangle \otimes |+\rangle], \tag{8}$$

$$|\mathrm{post}(0)\rangle = |\mathrm{post}(2)\rangle. \tag{9}$$

B. Pre- and post-selection paradox

Pre- and post-selection can lead to paradoxes [20], such as the three-box one [21]. In our case, the paradox originates from the following counterfactual reasoning [17]. Imagine that at time $t = 0$, the system was pre-selected in the state $|\mathrm{pre}(0)\rangle$, and at time $t = 2$, it was post-selected in the state $|\mathrm{post}(2)\rangle$. Now we ask: what if between pre-selection and post-selection somebody looked for the walker at a certain location? Interestingly, for some locations, the answers are deterministic, yet counterintuitive (hence the name *logical* pre- and post-selection paradox [22,23]). In particular, if at time $t = 0$ (or $t = 2$) one asked if the walker is at position $x = 0$, the answer would have to be YES. This is because if the answer was NO, the state $|\mathrm{pre}(0)\rangle$ ($|\mathrm{pre}(2)\rangle$) would collapse onto

$$|\mathrm{pre}_{\bar{0}}\rangle = \tfrac{1}{2}(|2\rangle + |4\rangle) \otimes (|-\rangle + |+\rangle). \tag{10}$$

The collapsed state cannot be later measured as $|\mathrm{post}(2)\rangle$, since $\langle \mathrm{pre}_{\bar{0}}|\mathrm{post}(2)\rangle = 0$. Therefore, the answer would have to be YES due to the post-selection assumption. Similarly, if at time $t = 1$ one asked if the walker is at position $x = 5$, the answer would have to be YES too. If the answer were NO, the state $|\mathrm{pre}(1)\rangle$ would collapse onto

$$|\mathrm{pre}_{\bar{5}}\rangle = \tfrac{1}{2}(|1\rangle + |3\rangle) \otimes (|-\rangle + |+\rangle), \tag{11}$$

which is orthogonal to $|\mathrm{post}(1)\rangle$. We conclude that at $t = 0$ and $t = 2$, the walker was at $x = 0$, and at $t = 1$, it was at $x = 5$. This is paradoxical since the model allows the walker to jump only to neighboring positions.

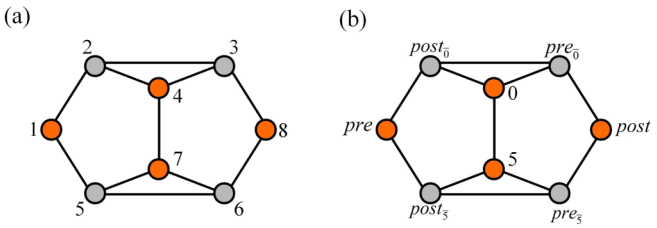

FIG. 1. A graph representing the Clifton's proof of contextuality. The vertices represent measurable events and the edges represent the exclusivity relation between the events. The events are assigned the logical values YES (orange) and NO (gray). In a NCHV theory, the logical values are assigned to all events, i.e., all vertices need to be colored either orange or gray. The graph structure implies the paradox (see explanation in the main text). (a) The eight Clifton's events. (b) The events in our quantum walk scenario.

C. Contextuality

The above is a LPPS paradox since the probabilities of counterfactual events are either zero or one. Such paradoxes were shown to be equivalent to proofs of contextuality [18,19]. Below we base on the work of Leifer and Spekkens [22] and relate the quantum walk LPPS paradox to the Clifton's proof of contextuality [24]. The Clifton's proof can be formulated with the help of a graph—see Fig. 1. The vertices in the graph correspond to measurable events, whereas the edges denote the exclusivity relation between them. This means that if one event happens, any other event connected to it by an edge cannot happen. The noncontextual hidden variable (NCHV) theory assigns the logical values YES and NO to all vertices (orange and gray color, respectively). This assignment represents an NCHV preparation of a system. The act of measurement in such a theory merely reveals the preassigned values. The value YES means that the corresponding event will be observed (when measured), whereas NO means that it will not.

Let us first consider a general scenario of eight events [Fig. 1(a)], $e = 1, 2, \ldots, 8$. We assume that the system is preselected in a state corresponding to the event 1 and

post-selected in a state corresponding to the event 8. This means that within a NCHV theory, the vertices 1 and 8 are assigned the logical values YES. However, such assignment implies that the events 2 and 5 (exclusive to 1) and events 3 and 6 (exclusive to 8) must be assigned NO. Finally, consider two mutually exclusive events, 4 and 7, such that 4 is complementary to 2 OR 3 and 7 is complementary to 5 OR 6. This means that if 2 and 3 are assigned NO, then 4 must be assigned YES. Similarly, if 5 and 6 are assigned NO, then 7 must be assigned YES. We obtained a contradiction since, due to exclusivity, 4 and 7 cannot both be assigned YES. Hence, the system cannot be described by a NCHV theory.

As shown by Clifton, it is possible to find a quantum system for which there exists a set of eight events whose exclusivity relations match the ones represented in the above graph. The event i corresponds to a projector Π_i. If two events i and j are exclusive, the corresponding projectors are orthogonal, $\Pi_i \Pi_j = 0$. This means that such quantum system does not admit a NCHV description.

Now we return to our quantum walk scenario. In particular, we are going to show that there are eight events in our system corresponding to the Clifton's events—see Fig. 1(b). Clearly, the events 1 and 8 correspond to projectors

$$\Pi_{\text{pre}} = |\text{pre}(0)\rangle\langle\text{pre}(0)| = |\text{pre}(2)\rangle\langle\text{pre}(2)| \tag{12}$$

and

$$\Pi_{\text{post}} = |\text{post}(0)\rangle\langle\text{post}(0)| = |\text{post}(2)\rangle\langle\text{post}(2)|. \tag{13}$$

The two exclusive events 4 and 7 correspond to quantum walk events in which at time $t = 0, 2$, the particle is at $x = 0$, and in which at time $t = 1$, the particle is at $x = 5$, respectively. In Fig. 1(b), these events are denoted as 0 and 5. They correspond to projectors

$$\Pi_0 = |0\rangle\langle 0| \otimes \mathbb{1}_c \tag{14}$$

and

$$\Pi_5 = U|5\rangle\langle 5| \otimes \mathbb{1}_c U^\dagger, \tag{15}$$

where $\mathbb{1}_c$ is the identity operator on the coin space and U is the unitary operator generating a single step of the evolution. The operator U is included in the projector Π_5 due to the fact that this measurement is done at time $t = 1$, i.e., after one step of the evolution. Note that $U^2 = \mathbb{1}$, and hence the evolution operator does not need to be included in projectors corresponding to measurements done at $t = 2$.

We are left with four Clifton's events: 2, 3, 5, and 6. The event 2, which we label $\text{post}_{\bar{0}}$, corresponds to a situation in which at time $t = 0, 2$, the particle's coin state is $|c_-\rangle \equiv \frac{1}{\sqrt{2}}(|-\rangle - |+\rangle)$ and its position is not $x = 0$. The associated projector is

$$\Pi_{\text{post}_{\bar{0}}} = (\mathbb{1}_x - |0\rangle\langle 0|) \otimes |c_-\rangle\langle c_-|, \tag{16}$$

where $\mathbb{1}_x$ is the identity operator in the position space. Note that this projector is orthogonal to both Π_{pre} and Π_0. In addition, since we consider a particular post-selection, effectively,

$$\Pi_{\text{post}_{\bar{0}}} = |\text{post}_{\bar{0}}\rangle\langle\text{post}_{\bar{0}}|, \tag{17}$$

where

$$|\text{post}_{\bar{0}}\rangle = \tfrac{1}{2}(|2\rangle + |4\rangle) \otimes (|-\rangle - |+\rangle). \tag{18}$$

Similarly, the event 5, which we label $\text{post}_{\bar{5}}$, corresponds to a situation in which at time $t = 1$, the particle's coin state is $|c_-\rangle$ and its position is not $x = 5$. The associated projector is

$$\Pi_{\text{post}_{\bar{5}}} = U(\mathbb{1}_x - |5\rangle\langle 5|) \otimes |c_-\rangle\langle c_-|U^\dagger. \tag{19}$$

It is orthogonal to both Π_{pre} and Π_5. Moreover, as before, due to post-selection, effectively,

$$\Pi_{\text{post}_{\bar{5}}} = U|\text{post}_{\bar{5}}\rangle\langle\text{post}_{\bar{5}}|U^\dagger, \tag{20}$$

where

$$U|\text{post}_{\bar{5}}\rangle = U\tfrac{1}{2}(|1\rangle + |3\rangle) \otimes (|+\rangle - |-\rangle). \tag{21}$$

Next, the event 3, labeled $\text{pre}_{\bar{0}}$, corresponds to a situation in which at time $t = 0, 2$, the particle's coin state is $|c_+\rangle \equiv \frac{1}{\sqrt{2}}(|-\rangle + |+\rangle)$ and its position is not $x = 0$. The associated projector,

$$\Pi_{\text{pre}_{\bar{0}}} = (\mathbb{1}_x - |0\rangle\langle 0|) \otimes |c_+\rangle\langle c_+|, \tag{22}$$

is orthogonal to $\Pi_{\text{post}_{\bar{0}}}$, Π_0, and Π_{post}. This time, the preselection implies that effectively,

$$\Pi_{\text{pre}_{\bar{0}}} = |\text{pre}_{\bar{0}}\rangle\langle\text{pre}_{\bar{0}}|, \tag{23}$$

where $|\text{pre}_{\bar{0}}\rangle$ is given in Eq. (10). Finally, the event 6, labeled $\text{pre}_{\bar{5}}$, corresponds to a situation in which at time $t = 1$, the particle's coin state is $|c_+\rangle$ and its position is not $x = 5$. The associated projector,

$$\Pi_{\text{pre}_{\bar{5}}} = U(\mathbb{1}_x - |5\rangle\langle 5|) \otimes |c_+\rangle\langle c_+|U^\dagger, \tag{24}$$

is orthogonal to $\Pi_{\text{post}_{\bar{5}}}$, Π_5, and Π_{post}. Once more, the preselection implies that effectively,

$$\Pi_{\text{pre}_{\bar{5}}} = U|\text{pre}_{\bar{5}}\rangle\langle\text{pre}_{\bar{5}}|U^\dagger, \tag{25}$$

where $|\text{pre}_{\bar{5}}\rangle$ is given in Eq. (11).

The above set of projectors, under the pre- and post-selection assumption, constitute a proof of contextuality in our quantum walk model. In the next section, we are going to transform it into an experimentally testable inequality.

D. Experimentally testable witness

The above proof of contextuality is a mathematical statement. It is not an experimentally realizable test. To make it testable in a laboratory, we transform it into an inequality that sets some noncontextual hidden variables (NCHVs) bound on a function of measurable data. If the inequality is violated, the tested system is confirmed to be contextual.

We first reduce the Clifton's proof to the Wright–Klyachko-Can-Binicioglu-Shumovsky (Wright-KCBS) scenario [25,26]. The system is prepared in the state $|\text{pre}(0)\rangle$, but only five out of eight measurement events are considered: $\text{pre}_{\bar{0}}$, 0, 5, $\text{pre}_{\bar{5}}$, post. These five events form a subgraph—a 5-cycle. The exclusivity relations in such a graph imply that at most, two events can be assigned a logical value YES, and hence in the NCHV theory, the following inequality must hold:

$$p(\text{pre}_{\bar{0}}) + p(0) + p(5) + p(\text{pre}_{\bar{5}}) + p(\text{post}) \leqslant 2, \tag{26}$$

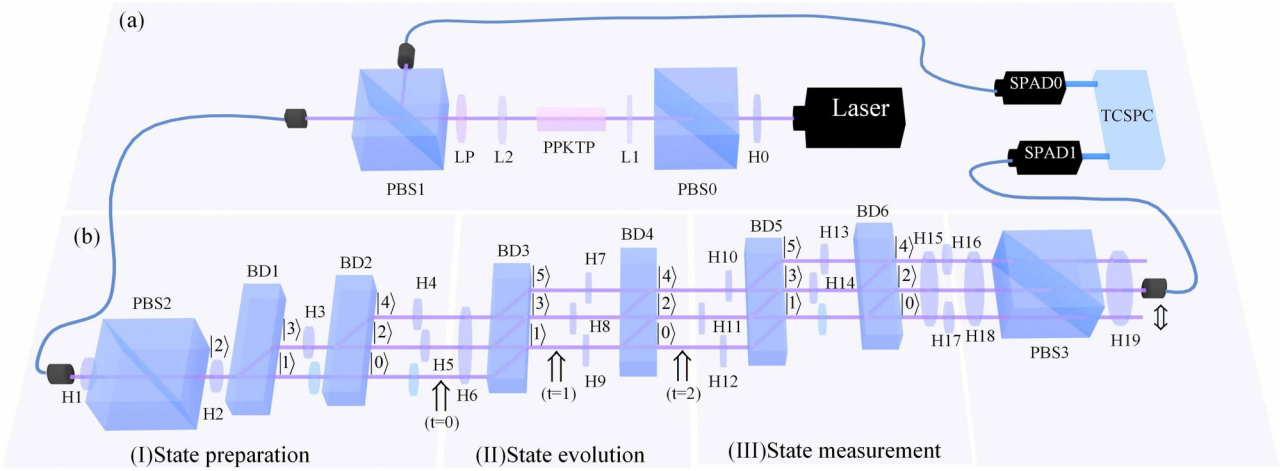

FIG. 2. Experimental setup. (a) Single-photon source preparation. A 405 nm continuous wave (CW) diode laser with 20 mW power pumps a periodically poled potassium titanyI phosphate (PPKTP) crystal to produce photon pairs with central wavelength of 810 nm based on SPDC. The H0 and PBS0 are used to regulate optical power. The two lenses (L1 and L2) before and after PPKTP are used for focusing and collimating beams, respectively. Then, after filtering out the pumped laser with a long pass filter (LP), the photon pairs are split on PBS1 and are coupled into single-mode fibers (SMF). (b) State preparation, state evolution, and state measurement. The numbers on the figure represent the position of the walker. The unlabeled blue objects in the figure are all glass plates used to compensate for the phase. Ideally, after BD6, only a HWP is needed on the path $|2\rangle$. However, in the experiment we used HWP15 that spanned three paths. Therefore, HWP16 and HWP17 are needed to ensure that the polarization of the $|0\rangle$ and $|4\rangle$ paths is in the $|V\rangle$ mode. Finally, we detect photons at the transmission end of PBS3 by adjusting HWP18 and HWP19. The quantum walk photons are detected by SPAD1, whereas the heralding photon is detected by SPAD0. The effective coincidence window (including the jitter of the detector) is about 2 ns.

where $p(X)$ denotes the probability that an event X happens.

The above inequality can be reformulated in terms of a correlation inequality [26]. One can define five binary ± 1 observables,

$$A_X = \mathbb{1} - 2\Pi_X, \tag{27}$$

where X: $\text{pre}_{\bar{0}}$, 0, 5, $\text{pre}_{\bar{5}}$, post. Note that the orthogonality between certain projectors implies joint measurability of the corresponding observables. The correlation inequality yields

$$\langle A_{\text{pre}_{\bar{0}}} A_0\rangle + \langle A_0 A_5\rangle + \langle A_5 A_{\text{pre}_{\bar{5}}}\rangle + \langle A_{\text{pre}_{\bar{5}}} A_{\text{post}}\rangle + \langle A_{\text{post}} A_{\text{pre}_{\bar{0}}}\rangle \geqslant -3. \tag{28}$$

For two operators A_X and A_Y that correspond to orthogonal projectors $\Pi_X \Pi_Y = 0$, we have

$$\langle A_X A_Y\rangle = \langle(\mathbb{1} - 2\Pi_X - 2\Pi_Y)\rangle = 1 - 2p(X) - 2p(Y). \tag{29}$$

Plugging this to (28) results in (26).

The DTQW scenario allows one to violate the above inequality (26) only up to $2 + \frac{1}{25}$. In addition, violation of such inequality would require implementation of joint or sequential measurements, which is demanding and introduces additional noise to the setup. Since we were unable to observe violation of (26) in our setup, we propose the following contextuality witness. We take advantage of the fact that in an ideal setting, $\{\text{pre}_{\bar{0}}, 0, \text{post}_{\bar{0}}\}$ and $\{\text{pre}_{\bar{5}}, 5, \text{post}_{\bar{5}}\}$ form a complete set of mutually exclusive events, and hence

$$p(\text{pre}_{\bar{0}}) + p(0) = 1 - p(\text{post}_{\bar{0}}), \tag{30}$$

$$p(\text{pre}_{\bar{5}}) + p(5) = 1 - p(\text{post}_{\bar{5}}). \tag{31}$$

Plugging the above into Eq. (26), we get the inequality

$$p(\text{post}) \leqslant p(\text{post}_{\bar{0}}) + p(\text{post}_{\bar{5}}), \tag{32}$$

which is a contextuality witness. This inequality can be tested in the laboratory and its violation would confirm that our quantum walk model is contextual. We stress that this confirmation is under the assumptions of NCHV and exclusivity (NCHV+E).

The pre-selection in the state $|\text{pre}(0)\rangle$ and post-selection in the state $|\text{post}(2)\rangle$ imply that one can evaluate the above probabilities in a relatively simple way. The probability $p(\text{post})$ is simply the probability of post-selection. On the other hand, the probabilities $p(\text{post}_{\bar{0}})$ and $p(\text{post}_{\bar{5}})$ are the probabilities of post-selection in situations in which the positions 0 and 5 are blocked, respectively. The theoretical estimation of these probabilities yields the violation

$$\tfrac{1}{25} \leqslant 0 + 0. \tag{33}$$

We confirmed this theoretical prediction in the single-photon quantum walk experimental scenario.

E. Experimental verification

We now demonstrate an experimental implementation of a one-dimensional single-photon DTQW and a violation of Eq. (32). The experimental setup is illustrated in Fig. 2, which is composed of four modules designed for single-photon source preparation, state preparation, state evolution, and state measurement (for more details, see Sec. III). In order to demonstrate a violation of Eq. (32), we use three versions of the setup.

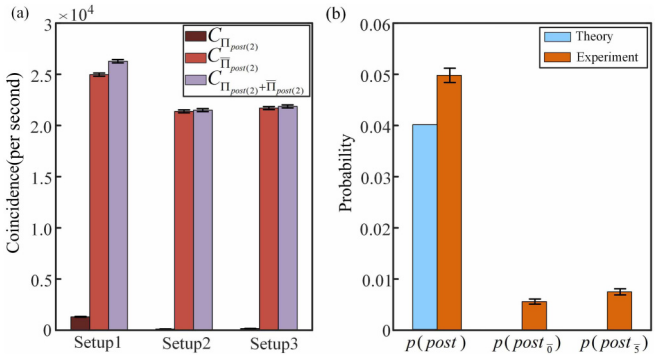

FIG. 3. Experimental results. (a) Coincidence photon counts. The distribution of the number of photons measured post-selection in three setups. The x coordinate represents the three experimental setups and the y coordinate represents the coincidence photon counts. Dark brown bars (in the first column) represent the coincidence photon counts between SPAD0 and the output of $\Pi_{\text{post}(2)}$. Red bars (in the second column) represent the coincidence photon counts between SPAD0 and the outputs of the complement of $\Pi_{\text{post}(2)}$, i.e., $\bar{\Pi}_{\text{post}(2)}$. Purple bars (in the third column) represent the total coincidence photon counts. (b) The probability distributions for the three setups. The plotted data are the raw data without subtraction of background counts. Error bars indicate statistical errors.

Setup 1: In the first setup, there is no path blocked. This allows us to evaluate the probability

$$p(\text{post}) = |\langle \text{post}(2)|\text{pre}(2)\rangle|^2. \tag{34}$$

Setup 2: In the second setup, the position $x = 0$ is blocked at time $t = 0$. Therefore, we can evaluate the probability

$$p(\text{post}_{\bar{0}}) = |\langle \text{post}(2)|\text{pre}_{\bar{0}}(2)\rangle|^2. \tag{35}$$

Setup 3: In the third setup, the position $x = 5$ is blocked at time $t = 1$. Hence, we can evaluate the probability

$$p(\text{post}_{\bar{5}}) = |\langle \text{post}(2)|\text{pre}_{\bar{5}}(2)\rangle|^2. \tag{36}$$

As shown in Fig. 3, these are the experimental results. Figure 3(a) represents the coincidence photon counts. All the data shown in the figure are raw data (without removing background noise). The post-selection measurement probabilities are shown in Fig. 3(b) and the values obtained are

$$p(\text{post}) = \frac{C_{\Pi_{\text{post}(2)}}}{C_{\Pi_{\text{post}(2)}+\bar{\Pi}_{\text{post}(2)}}} = 0.0498 \pm 0.0014 \quad \text{(setup 1)}, \tag{37}$$

$$p(\text{post}_{\bar{0}}) = \frac{C_{\Pi_{\text{post}(2)}}}{C_{\Pi_{\text{post}(2)}+\bar{\Pi}_{\text{post}(2)}}} = 0.0056 \pm 0.0005 \quad \text{(setup 2)}, \tag{38}$$

$$p(\text{post}_{\bar{5}}) = \frac{C_{\Pi_{\text{post}(2)}}}{C_{\Pi_{\text{post}(2)}+\bar{\Pi}_{\text{post}(2)}}} = 0.0075 \pm 0.0006 \quad \text{(setup 3)}. \tag{39}$$

In the above, $C_{\Pi_{\text{post}(2)}}$ denotes the number of coincidence counts for which the {\rm post}-selection happened and $C_{\Pi_{\text{post}(2)}+\bar{\Pi}_{\text{post}(2)}}$ denotes the total number of coincidence counts.

It is obvious that these experimentally measured probabilities violate Eq. (32),

$$\begin{aligned} p(\text{post}) &= 0.0498 \pm 0.0014 \\ &\nleq p(\text{post}_{\bar{0}}) + p(\text{post}_{\bar{5}}) = 0.0131 \pm 0.0011. \end{aligned} \tag{40}$$

It can be noted that within the limits of experimental errors, we can still get a violation of Eq. (32). The imperfection of the experiment is mainly due to a systematic error caused by the limited precision of wave plates and the imperfect visibility of Mach-Zehnder interferometers. Since the single-photon detection efficiency is not high, we must adopt the fair sampling hypothesis, which is a standard assumption in experiments of this type.

III. METHODS

A. Single-photon generation

As shown in Fig. 2(a), in the spontaneous parametric down-conversion (SPDC), the pairs of orthogonally polarized photons are produced in a polarization product state. We separate them at the polarizing beam splitter 1 (PBS1). A detection of a vertically polarized photon at SPAD0 heralds a horizontally polarized photon in our setup [27]. Similar to [28], we first conduct the Hanbury Brown-Twiss (HBT) experiment to confirm that the light source used in our experiment is a single-photon source. In Fig. 4, a clear dip represents the minimum value of $g^{(2)} = 0.0293$. This confirms that our source is indeed a single-photon source.

B. Experimental DTQW setup

The photonic DTQW setup consists of three parts, shown in Fig. 2(b). In the state preparation part, we use the half-wave plate 1 (HWP1, referred to as H1) and the PBS2 to regulate the light power and to ensure that the input light in the subsequent system is horizontally polarized. The two degrees of freedom, i.e., the single-photon polarization and the path, are used to encode the coin states $|\pm\rangle$ and the position states $|x\rangle$ of the walker, respectively. To prepare the initial state, we use beam displacers (BDs) and HWPs. BDs transmit vertically

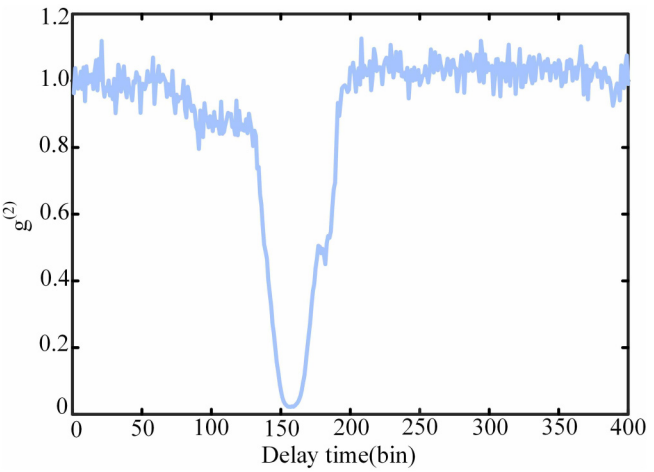

FIG. 4. Second-order correlation of a single-photon source. There is a clear dip in 160 time bins and every bin is 64 ps.

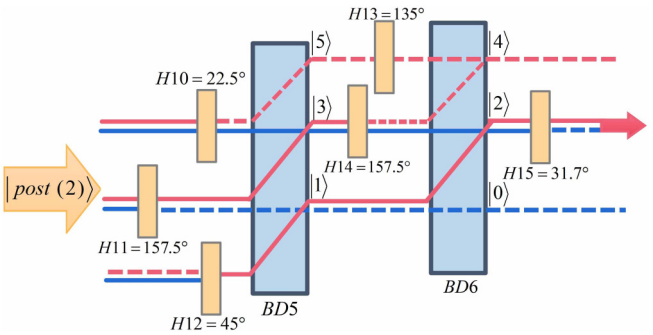

FIG. 5. Experimental setup for measuring a single observable. $|\text{post}(2)\rangle$ [$|\text{post}(\bar{2})\rangle$, which represents the orthogonal of $|\text{post}(2)\rangle$] is the eigenstate of $\Pi_{\text{post}(2)}$ corresponding to the eigenvalue -1 [$+1$]. The number accompanying each HWP is the angle of its optical axis relative to the horizontal polarization direction. The red line represents the $|H\rangle$ polarization in the path, and the blue line represents the $|V\rangle$ polarization. The red (blue) dotted line shows that there is no photon in the $|H\rangle$ polarization ($|V\rangle$ polarization) of this path.

polarized photons and displace horizontally polarized ones. Initially, the system's state is $|2\rangle \otimes |H\rangle$. After HWP2–HWP5, BD1, and BD2, it becomes

$$|\text{pre}(0)\rangle = \frac{1}{\sqrt{5}}[|0\rangle \otimes |V\rangle + (|2\rangle + |4\rangle) \otimes (|V\rangle + |H\rangle)]. \tag{41}$$

The above state corresponds to Eq. (3). This ends the preparation (pre-selection) stage.

In the state evolution part, the unitary operator generating a single step is realized via a combination of HWPs and BDs. The elements H6 and BD3 evolve the system from $t = 0$ to $t = 1$. The resulting state is

$$|\text{pre}(1)\rangle = \frac{1}{\sqrt{5}}[(|1\rangle + |3\rangle) \otimes (|V\rangle + |H\rangle) + |5\rangle \otimes |H\rangle], \tag{42}$$

which corresponds to Eq. (4). Similarly, HWP7–HWP9 and BD4 are used to evolve the system from $t = 1$ to $t = 2$. The system's state returns to $|\text{pre}(0)\rangle$ [since $|\text{pre}(2)\rangle = |\text{pre}(0)\rangle$].

In the last part, we measure (post-select) the system in the state

$$|\text{post}(2)\rangle = \frac{1}{\sqrt{5}}[|0\rangle \otimes |V\rangle + (|2\rangle + |4\rangle) \otimes (|V\rangle - |H\rangle)] \tag{43}$$

that corresponds to Eq. (6). Therefore, we need to design a proper measurement device. According to [29], it is a typical single-observable measuring devices (see Fig. 5). The settings of HWP10–HWP15 are chosen to transform the state $|\text{post}(2)\rangle$ onto $|2\rangle \otimes |H\rangle$. The angles of all the HWPs used above are shown in Table I (see more details in the Supplemental Material [30]). Finally, output photons are detected using a single-photon detector that consists of a single-photon avalanche photodiode (SPAD) and time-correlated single-photon counting (TCSPC). We register coincidences between SPAD1 (D1) and the trigger SPAD0 (D0). For each measurement, we record clicks for 1 s, registering about 11 000 heralded single photons.

TABLE I. Setting angles of the wave plates for realizing the total experimental setup.

HWP	HWP2	HWP3	HWP4	HWP5
θ	13.3°	157.5°	22.5°	157.5°
HWP	HWP6	HWP7	HWP8	HWP9
θ	45°	45°	45°	45°
HWP	HWP10	HWP11	HWP12	HWP13
θ	22.5°	157.5°	45°	135°
HWP	HWP14	HWP15	HWP16	HWP17
θ	157.5°	31.7°	−58.3°	−58.3°

IV. DISCUSSION

In this paper, we have proposed a LPPS paradox based on a DTQW. Namely, we showed that under pre- and post-selection assumption, a single-photon DTQW undergoes a nonclassical long distance oscillation. Next, we related this paradox to the Clifton's proof of contextuality. Then, we transformed this proof into a Bell-like inequality, whose violation confirms contextuality of the underlying system. Finally, we used an exclusivity assumption and transformed the inequality into a contextuality witness. We experimentally implemented a single-photon DTQW and confirmed contextuality in our system up to 8 standard deviations. Therefore, we confirmed that DTQWs cannot be described by a noncontextual hidden variable theory under the assumption that outcomes of certain measurements are exclusive.

ACKNOWLEDGMENTS

This work is supported by National Key R&D Program of China (Grant No. 2018YFB0504300). At the early stage of research, T.K. and P.K. were supported by the Ministry of Science and Higher Education in Poland (science funding scheme 2016-2017, Project No. 0415/IP3/2016/74). At the final stage of research, P.K. was supported by the Polish National Science Centre (NCN) under the Maestro Grant No. DEC-2019/34/A/ST2/00081.

[1] Y. Aharonov, L. Davidovich, and N. Zagury, Quantum random walks, Phys. Rev. A **48**, 1687 (1993).

[2] D. A. Meyer, From quantum cellular automata to quantum lattice gases, J. Stat. Phys. **85**, 551 (1996).

[3] J. Kempe, Quantum random walks - An introductory overview, Cont. Phys. **44**, 307 (2003).

[4] V. Kendon, Decoherence in quantum walks - A review, Math. Struct. Comput. Sci. **17**, 1169 (2007).

[5] D. Reitzner, D. Nagaj, and V. Buzek, Quantum walks, Acta Phys. Slovaca **61**, 603 (2011).
[6] S. E. Venegas-Andraca, Quantum walks: A comprehensive review, Quantum Inf. Proc. **11**, 1015 (2012).
[7] P. L. Knight, E. Roldan and J. E. Sipe, Quantum walk on the line as an interference phenomenon, Phys. Rev. A **68**, 020301(R) (2003).
[8] H. Jeong, M. Paternostro and M. S. Kim, Simulation of quantum random walks using the interference of a classical field, Phys. Rev. A **69**, 012310 (2004).
[9] S. K. Goyal, F. S. Roux, A. Forbes and T. Konrad, Implementing Quantum Walks Using Orbital Angular Momentum of Classical Light, Phys. Rev. Lett. **110**, 263602 (2013).
[10] B. Sephton *et al.*, A versatile quantum walk resonator with bright classical light, PLoS One **14**, e0214891 (2019).
[11] M. Markiewicz, D. Kaszlikowski, P. Kurzyński, and A. Wójcik, npj Quantum Inf. **5**, 5 (2019).
[12] A. Fine, Hidden Variables, Joint Probability, and the Bell Inequalities, Phys. Rev. Lett. **48**, 291 (1982).
[13] J. S. Bell, On the Einstein-Podolsky-Rosen paradox, Physics **1**, 195 (1964).
[14] S. Kochen and E. P. Specker, The problem of hidden variables in quantum mechanics, J. Math. Mech. **17**, 59 (1967).
[15] A. J. Leggett and A. Garg, Quantum Mechanics versus Macroscopic Realism: Is the Flux there When Nobody Looks? Phys. Rev. Lett. **54**, 857 (1985).
[16] C. Robens, W. Alt, D. Meschede, C. Emary and A. Alberti, Ideal Negative Measurements in Quantum Walks Disprove Theories Based on Classical Trajectories, Phys. Rev. X **5**, 011003 (2015).
[17] T. Kopyciuk, M. Lewandowski, P. Kurzyński, Pre- and post-selection paradoxes in quantum walks, New J. Phys. **21**, 103054 (2019).
[18] M. F. Pusey, Anomalous Weak Values are Proofs of Contextuality, Phys. Rev. Lett. **113**, 200401 (2014).
[19] M. F. Pusey and M. S. Leifer, Logical pre- and post-selection paradoxes are proofs of contextuality, in *Proceeding 12th International Workshop on Quantum Physicsand Logic (QPL2015)*, Vol. 195, p. 295.
[20] Y. Aharonov, P. G. Bergmann and J. L. Lebowitz, Time symmetry in the quantum process of measurement, Phys. Rev. **134**, B1410 (1964).
[21] Y. Aharonov and L. Vaidman, Complete description of a quantum system at a given time, J. Phys. A: Math. Gen. **24**, 2315 (1991).
[22] M. S. Leifer and R. W. Spekkens, Pre- and Post-Selection Paradoxes and Contextuality in Quantum Mechanics, Phys. Rev. Lett. **95**, 200405 (2005).
[23] M. S. Leifer and R. W. Spekkens, Logical pre- and post-selection paradoxes, measurement-disturbance and contextuality, Intl. J. Theor. Phys. **44**, 1977 (2005).
[24] R. Clifton, Getting contextual and nonlocal elements-of-reality the easy way, Am. J. Phys. **61**, 443 (1993).
[25] R. Wright, in *Mathematical Foundations of Quantum Mechanics*, edited by A. R. Marlow (Academic, San Diego, 1978), p. 255.
[26] A. A. Klyachko, M. A. Can, S. Binicioglu and A. S. Shumovsky, Simple Test for Hidden Variables in Spin-1 Systems, Phys. Rev. Lett. **101**, 020403 (2008).
[27] J. Z. Yang, M. F. Li, X. X. Chen, W. K. Yu and A. N. Zhang, Single-photon quantum imaging via single-photon illumination, Appl. Phys. Lett. **117**, 214001 (2020).
[28] X. X. Chen, J. Z. Yang, X. D. Chai, and A. N. Zhang, Single-photon Bell state measurement based on a quantum random walk, Phys. Rev. A **100**, 042302 (2019).
[29] Y. F. Huang, M. Li, D. Y. Cao, C. Zhang, Y. S. Zhang, B. H. Liu, C. F. Li and G. C. Guo, Experimental test of state-independent quantum contextuality of an indivisible quantum system, Phys. Rev. A **87**, 052133 (2013).
[30] See Supplemental Material at http://link.aps.org/supplemental/10.1103/PhysRevA.104.012220 for more details on how to set the angle of half-wave plates in state preparation, state evolution and state measurement. The Supplemental Material includes Refs. [28,29].